Wake Fields in 9-Cell TESLA Accelerating Structures: Spectral Element Discontinuous Galerkin (SEDG) Simulations*

Misun Min,†‡ Paul F. Fischer, ‡ Yong-Chul Chae,§
‡Mathematics and Computer Science, Argonne National Laboratory, Argonne, IL 60439, USA
§Advanced Photon Source, Argonne National Laboratory, Argonne, IL 60439, USA

Abstract

Using our recently developed high-order accurate Maxwell solver, NEKCEM, we carried out longitudinal wakefields calculations for a 9-cell TESLA cavity structure in 3D. Indirect calculations are used for wake potentials. Computaional results by NEKCEM are demonstrated in comparison with GdfidL.

INTRODUCTION

NEKCEM employs spectral element discontinuous Galerkin (SEDG) method which is based on domain decomposition approach using spectral element discretizations on Gauss-Lobatto-Legendre grids with body-conforming hexahedral meshes [1]. The numerical scheme is designed to ensure high-order spectral accuracy [2, 4], using the discontinuous Galerkin form with boundary conditions weakly enforced through a flux term between elements. Concerns related to implementation on wake potential calculations are discussed, and wake potential calculations with indirect method by NEKCEM [3] are demonstrated in comparison with the results by a finite difference time-domain code, GdfidL.

FORMULATIONS

Governing equations to study beam dynamics and numerical discretizations in space and time are describded as follows.

Maxwell's Equations

We begin with the Maxwell equations:

$$\mu\frac{\partial H}{\partial t} = -\nabla\times E, \quad \epsilon\frac{\partial E}{\partial t} = \nabla\times H - J \tag{1}$$

$$\nabla\cdot E = \frac{\rho}{\epsilon}, \quad \nabla\cdot H = 0, \tag{2}$$

where the current source $J = (0, 0, J_z)$ is defined for an ultra-relativistic on-axis Gaussian beam moving in the z-direction:

$$J_z = c\rho(x,y)\rho(z-ct), \tag{3}$$

$$\rho(x,y) = \frac{1}{\sigma_r\sqrt{2\pi}}\exp\left(-\frac{x^2+y^2}{2\sigma_r^2}\right), \tag{4}$$

$$\rho(z) = \frac{1}{\sigma_z\sqrt{2\pi}}\exp\left(-\frac{z^2}{2\sigma_z^2}\right). \tag{5}$$

Conservation Form

We rewrite equation (1) into a conservation form

$$Q\frac{\partial q}{\partial t} + \nabla\cdot F(q) = -J, \tag{6}$$

where

$$q = (H_x, H_y, H_z, E_x, E_y, E_z)^T, \tag{7}$$

$$Q = diag(\mu,\mu,\mu,\epsilon,\epsilon,\epsilon), \tag{8}$$

and the flux $F(q)$ in the following form,

$$\begin{bmatrix} 0 & E_z & -E_y & 0 & -H_z & H_y \\ -E_z & 0 & E_x & H_z & 0 & -H_x \\ E_y & -E_x & 0 & -H_y & H_x & 0 \end{bmatrix}^T. \tag{9}$$

Numerical Discretizations

We seek a numerical solution $\mathbf{q_N}$, satisfying

$$\left(Q\frac{\partial \mathbf{q_N}}{\partial t} + \nabla\cdot F(\mathbf{q_N}) + J, \phi\right)_{\Omega^e} = (\hat{n}\cdot[F-F^*], \phi)_{\partial\Omega^e}, \tag{10}$$

where $\phi = L_i(x)$ is a local discontinuous test function and the numerical flux F^* is defined as in [2]. In the computational domain Ω as a set of body-conforming, nonoverlapping hexahedral meshes Ω^e, we define the local solution $\mathbf{q_N}$ on each Ω^e as

$$\mathbf{q_N}(x,t) = \sum_{j=0}^{N} q_j(t)L_j(x), \tag{11}$$

where $q_j(t)$ is the solution at N grid points x_j on Ω^e, and $L_j(x)$ is the three-dimensional Legendre Lagrange interpolation polynomial associated with the N-nodes [1]. Plugging (11) into the weak formulation (10 and taking Gauss quadrature for the integration, we obtain semi-discrete formulation of the scheme. Then we apply the fourth-order Runge-Kutta method for time integration.

Initial and Boundary Conditions

Initial fields are computed numerically for the ingoing pipe. For boundary conditions, we apply the uniaxial perfectly matched layer (UPML) [5] in the longitudinal direction and the perfectly electric conducting (PEC) boundary [2] for the transverse direction.

* Work supported by the U.S. Dept. of Energy under Contract DE-AC02-06CH11357.

† mmin@mcs.anl.gov

COMPUTATIONAL RESULTS

We demonstrate 9-cell TESLA mesh, and its wake potentials for various bunch sizes at different radius. Results are compared to GdfidL for the case of bunch size $\sigma_z = 5$ mm. Parallel efficiency of NEKCEM is also discussed.

TESLA Cavity with Spectral Element Mesh

We built a 9-Cell TESLA mesh shown in Figure 1, following the unit as in [6]. In transverse direction, meshes are scaled for radius grater than 26mm. Within the radius 26 mm, wake potentials are calculated along mesh surface in three dimensions.

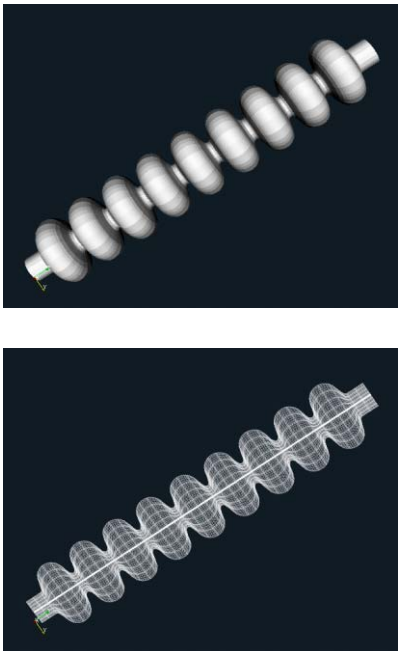

Figure 1: 9-Cell TESLA Mesh (top); Spectral Element Discretization (bottom).

Wake Potential

We compute the longitudinal wake potential defined as

$$W_z(x,y,s) = -\frac{1}{\mathcal{Q}} \int_{-\infty}^{\infty} E_z(x,y,z,t)dz, \qquad (12)$$

where $\mathcal{Q}$ is the total charge of a beam and

$$s = ct - z. \qquad (13)$$

Figure 2 shows wake potentials for different bunch sizes with a fixed polynomial degree $N = 5$ and the number of element $E = 1,368$. The behaviors of the wake potential profiles show reasonable profiles for the bunche sizes 3 mm, 4 mm and 5 mm.

Since we use indirect method for wake potential calculations, we examine how the wake potential profiles change at different radius. Figure 3 shows wake potential profiles at radius 26.0 mm and 19.25 mm for bunch size 5 mm with the degree of polynomial $N = 5$ and the number of element $E = 1,368$. The discrepancy for the cases between the 26.0 mm and 19.25 mm are shown on the unstructured grids unlike the case on the finite difference grids. Further Study has to be done with relatively even and finer meshes for the unstructured mesh case.

Figure 4 shows comparisons of the wake potentials for the bunch size 5mm beteen the Gdfdl and the SEDG. For the SEDG, the dashed line shows the case for $N = 7$ and solid line for $N = 5$. Discrepancy is observed on the results between GdfidL and SEDG. Further Study has to be carried out by changing the meshes and resolutions for the unstructured mesh case.

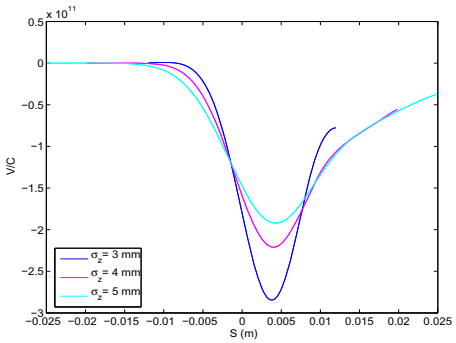

Figure 2: Wake potentials on the surface at $r = 26.0$mm for $\sigma_z = 3$, $\sigma_z = 4$ mm and $\sigma_z = 5$ mm. $\sigma_r = 1$mm.

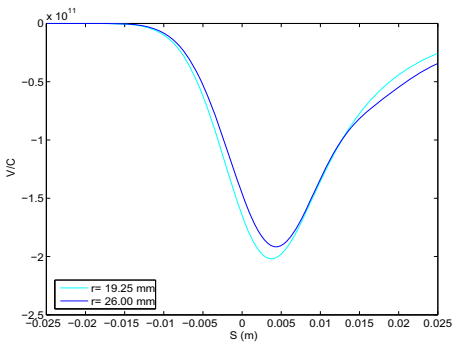

Figure 3: Wake potentials on the surface at $r = 26.0$ mm and $r = 19.25$ mm for $\sigma_z = 1$ mm and $\sigma_r = 1$ mm.

Parallel Efficiency

Figure 5 demonstrate the scaling of 3D computations of NEKCEM. The vertical axis is CPU time per time step, per grid point, per processor. The number of elements is fixed at $E = 512$ (8^3). The polynomial degrees varies from $N = 5$ to 10. Simulations were run on the number of processor, $P = 2^k$, $k = 0, \ldots, 7$, on the linux cluster, Jazz, at Argonne. The coarsest computations involve $n = 64,000$ points, which yields roughly 100 points per processor for the $P = 128$ case. Each curve shows some

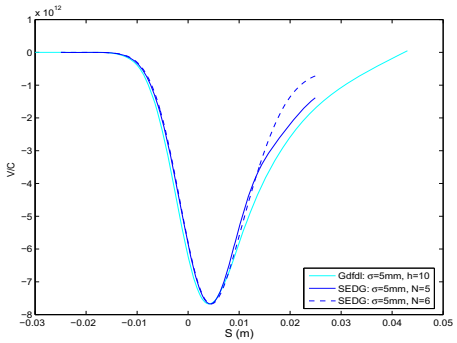

Figure 4: Wake potentials on the surface at $r = 26.0$mm for $\sigma_z = 5$ mm and $\sigma_r = 1$ mm on the meshes.

loss of parallel efficiency as the number of processors is increased - the CPU time increases from right ($P = 1$) to left ($P = 128$) on the graph. However, below approximately 3000 to 10,000 points per processor the CPU time actually *decreases* with super-linear speed-up.

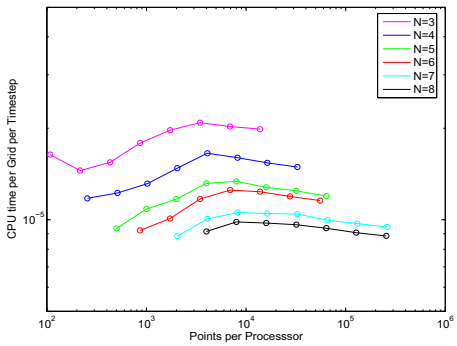

Figure 5: CPU time per grid point per time step per processor for 512 spectral elements with N ranging from 5 to 10, as a function of number of points per processor on Jazz.

CONCLUSIONS

We have applied the spectral element discontinuous Galerkin method to simulate beam dynamics within a three-dimensional 9-cell TESLA cavity. The wake potential calculations show resonable profiles depending on the bunch size. We showed comparisons on the wake potential calculations with Gdfdl results. We observe some discrepancy in the wake potential profiles by SEDG compared to the cases in GdfidL. Further study will be carried out regarding on the mesh refinement and resolution as a first step towards one picosecond bunch simulations.

REFERENCES

[1] M.O. Deville, P.F. Fischer, and E.H. Mund, "High Order Methods for Incompressible Fluid Flow," Cambridge University Press (2002).

[2] J.S. Hesthaven and T. Warburton,"Nodal High Order Methods on Unstructured Grids - I. Time-Domain Solution of Maxwell's Equations," J. Comp. Physics, 101 (2002), p. 186.

[3] M.S. Min and P.F. Fischer, "NEKCEM," Mathematics and Computer Science Division, Argonne National Laboratory. http://mercurial.mcs.anl.gov/nekcem/.

[4] M.S. Min, P.F. Fischer, and Y.C. Chae, "Spectral element discontinuous Galerkin simulations for wake potential calculations: NEKCEM," Proc. of Particle Accelerator Conference, 2007.

[5] A. Taflov and S.C. Hagness, "Computational Electromagnetics: The Finite-Difference Time Domain Method," Artech House, 3rd ed. (2005).

[6] R. Wanzenburg, "Monopole, Dipole and Quadrupole Passbands of the TESLA 9-cell Cavity," TESLA 2001-33, DESY, 2001.